

Suppression of persistent photoconductivity in high gain Ga_2O_3 Schottky photodetectors

Haitao Zhou(周海涛), Lujia Cong(丛璐佳), Jiangang Ma(马剑钢), Bingsheng Li(李炳生), Haiyang Xu(徐海洋), and Yichun Liu(刘益春)

Citation: Chin. Phys. B, 2021, 30 (**12**): 126104. DOI: 10.1088/1674-1056/ac2d1b
Journal homepage: http://cpb.iphy.ac.cn; http://iopscience.iop.org/cpb

What follows is a list of articles you may be interested in

Oxygen vacancies and V co-doped Co_3O_4 prepared by ion implantation boosts oxygen evolution catalysis

Bo Sun(孙博), Dong He(贺栋), Hongbo Wang(王宏博), Jiangchao Liu(刘江超), Zunjian Ke(柯尊健), Li Cheng(程莉), and Xiangheng Xiao(肖湘衡)

Chin. Phys. B, 2021, 30 (**10**): 106102. DOI: 10.1088/1674-1056/ac1339

Intrinsic luminescence centers in γ- and ϑ-alumina nanoparticles

Abdolvahab Amirsalari, Saber Farjami Shayesteh, Reza Taheri Ghahrizjani

Chin. Phys. B, 2017, 26 (**3**): 036101. DOI: 10.1088/1674-1056/26/3/036101

Influences of neutral oxygen vacancies and E_1'centers on α-quartz

Li Hui-Ran, Cheng Xin-Lu, Zhang Hong, Zhao Feng

Chin. Phys. B, 2015, 24 (**10**): 106105. DOI: 10.1088/1674-1056/24/10/106105

Bipolar tri-state resistive switching characteristics in Ti/CeO_x/Pt memory device

M. Ismail, M. W. Abbas, A. M. Rana, I. Talib, E. Ahmed, M. Y. Nadeem, T. L. Tsai, U. Chand, N. A. Shah, M. Hussain, A. Aziz, M. T. Bhatti

Chin. Phys. B, 2014, 23 (**12**): 126101. DOI: 10.1088/1674-1056/23/12/126101

Oxygen vacancy-induced room-temperature ferromagnetism in D-D neutron irradiated single-crystal TiO_2 (001) rutile

Xu Nan-Nan, Li Gong-Ping, Pan Xiao-Dong, Wang Yun-Bo, Chen Jing-Sheng, Bao Liang-Man

Chin. Phys. B, 2014, 23 (**10**): 106101. DOI: 10.1088/1674-1056/23/10/106101

Suppression of persistent photoconductivity in high gain Ga_2O_3 Schottky photodetectors*

Haitao Zhou(周海涛), Lujia Cong(丛璐佳), Jiangang Ma(马剑钢)†, Bingsheng Li(李炳生), Haiyang Xu(徐海洋), and Yichun Liu(刘益春)

Key Laboratory for UV-Emitting Materials and Technology of Ministry of Education, Northeast Normal University, Changchun 130024, *China*

(Received 7 July 2021; revised manuscript received 25 August 2021; accepted manuscript online 6 October 2021)

The defect-related photoconductivity gain and persistent photoconductivity (PPC) observed in Ga_2O_3 Schottky photodetectors lead to a contradiction between high responsivity and fast recovery speed. In this work, a metal–semiconductor–metal (MSM) Schottky photodetector, a unidirectional Schottky photodetector, and a photoconductor were constructed on Ga_2O_3 films. The MSM Schottky devices have high gain (> 13) and high responsivity (> 2.5 A/W) at 230–250 nm, as well as slow recovery speed caused by PPC. Interestingly, applying a positive pulse voltage to the reverse-biased Ga_2O_3/Au Schottky junction can effectively suppress the PPC in the photodetector, while maintaining high gain. The mechanisms of gain and PPC do not strictly follow the interface trap trapping holes or the self-trapped holes models, which is attributed to the correlation with ionized oxygen vacancies in the Schottky junction. The positive pulse voltage modulates the width of the Schottky junction to help quickly neutralize electrons and ionized oxygen vacancies. The realization of suppression PPC functions and the establishment of physical models will facilitate the realization of high responsivity and fast response Schottky devices.

Keywords: Ga_2O_3 Schottky photodetector, persistent photoconductivity, high gain, pulse voltage, oxygen vacancy

PACS: 61.72.jd, 73.30.+y, 85.60.Dw, 85.30.De **DOI:** 10.1088/1674-1056/ac2d1b

1. Introduction

Recently, Ga_2O_3 and related materials have attracted widespread attention due to their potential applications in optoelectronic and microelectronic devices.[1–9] Although significant progress has been made in the research of Ga_2O_3 based devices, the manipulation and understanding of its defects and related physical characteristics still demand further research,[10–18] for example, the defect-related photoconductivity gain and persistent photoconductivity (PPC) observed in Ga_2O_3 photodetectors.[19–25] The photoconductive gain increases the responsivity of the device, which is conducive to the detection of weak light, while PPC increases the response recovery time of the device, which is not conducive to the detection of high-frequency switching light. In photodetectors based on ZnO, SnO_2, InGaZnO, and GaN, the application of "interference" (for example, bending, illumination, heating and electric field) to suppress PPC in the photodetector has been proven to be efficient and feasible without affecting the high responsivity (gain).[26–31] Recently, heating and electric fields have been used in Ga_2O_3 photodetectors to maintain high gain and effectively suppress PPC. In our previous work,[21] we studied the effect of "short-time heating" process on PPC in Ga_2O_3 photoconductor, through which the PPC can be effectively suppressed within a few seconds. From an application point of view, the electric field may be more capable of suppressing PPC in microseconds. Han *et al.*[22] and Ahn *et al.*[24] adopted the method proposed by Jeon *et al.*[26] to suppress PPC in Ga_2O_3 three-terminal transistor by applying a pulse voltage at gate. Qiao *et al.*[31] suppressed PPC in $Si/Al_2O_3/Ga_2O_3$ heterojunction photodetectors by applying a pulse voltage. However, there is no report on the effect of the pulse voltage on PPC in a simple two-terminal Ga_2O_3 Schottky photodetector.

In this paper, the metal–semiconductor–metal (MSM) Schottky Ga_2O_3 photodetectors we prepared show high gain and PPC. We study the influence of pulse voltage size and width on PPC in MSM Schottky Ga_2O_3 photodetectors. Combining the photoresponse characteristics of the prepared Ga_2O_3 photoconductors and the unidirectional Schottky devices and the effect of pulse voltage on the PPC, a physical model related to ionized oxygen vacancies in the reverse-biased Schottky junction is proposed.

2. Experimental methods

Ga_2O_3 films were grown on *c*-plane sapphire substrates at room temperature by pulsed laser deposition (PLD). The substrates were sequentially cleaned with acetone, ethanol and deionized water in an ultrasonic bath for 10 min, respectively.

*Project supported by the National Natural Science Foundation of China (Grant Nos. 51872043, 51732003, and 51902049), the National Key R&D Program of China (Grant No. 2019YFA0705202), Natural Science Foundation of Jilin Province, China (Grant No. 20200201076JC), the National Basic Research Program of China (Grant No. 2012CB933703), and "111" Project (Grant No. B13013).

†Corresponding author. E-mail: majg@nenu.edu.cn

© 2021 Chinese Physical Society and IOP Publishing Ltd

After being cleaned, the substrates were blown dry using nitrogen gas. The distance between the substrate and the target is 4.5 cm. The background pressure and oxygen pressure in the growth chamber were fixed at 1×10^{-6} Pa and 3×10^{-3} Pa, respectively. The Kr excimer laser pulse energy and repetition rate were 240 mJ and 10 Hz. The as-grown Ga_2O_3 films were subsequent thermally annealed at 600 °C in oxygen ambient. The crystal structures were characterized by a Rigaku D/max-2500 x-ray diffractometer. The optical characteristics were measured by a Hitachi UH4150 spectrometer. The morphologies were characterized by scanning electron microscopy (SEM, Hitachi S-4800). Al and Au electrodes were deposited on the annealed Ga_2O_3 films using shadow masks by vacuum thermal evaporation. The width, length and distance of the interdigital fingers in Au/Ga_2O_3/Au and Al/Ga_2O_3/Al devices are 50 μm, 1000 μm and 20 μm, respectively. The distance between the Au and Al square electrodes is 500 μm for the Au/Ga_2O_3/Al devices. The *I*–*V* characteristics and time-dependent photoresponse of the devices were measured using a Keithley 2461 sourcemeter and a system composed of a Xe lamp, a monochromator and an optical chopper.

3. Results and discussion

The XRD pattern of the Ga_2O_3 film is shown in Fig. 1(a). There are three diffraction peaks at 19.2°, 38.3°, and 59.3°, corresponding to the (-201), (-402) and (-603) crystal planes of β-Ga_2O_3, respectively.[32,33] However, the intensity ratio of (-201) and (-402) diffraction peaks is 0.031, which is lower than the theoretical value (2.2) reported in the literature.[34] This phenomenon may be caused by the overlap of the (0006) diffraction peak of α-Ga_2O_3 and the (-402) diffraction peak of β-Ga_2O_3.[34] Therefore, our Ga_2O_3 film may be a mixed-phase material with α (rhombohedral) and β (monoclinic) phases coexisting, and similar results have been reported by other research groups.[35,36] The thickness of the Ga_2O_3 film is about 290 nm, as shown in the cross-sectional image in the inset of Fig. 1(a).

Figure 1(b) shows the optical transmission spectrum of the Ga_2O_3 film. The spectrum shows a high transmittance of over 90% in the 300–800 nm, and has a cutoff at approximately 268 nm. The fitting result of the optical band-gap of the film is about 4.6 eV, as shown in the inset of Fig. 1(b). The optical band gap obtained here is consistent with the results (4–4.7 eV) reported in the literature by the PLD method at a relatively low preparation temperature (< 650 °C).[37,38] However, it is slightly smaller than the previously reported 4.8–5.1 eV.[39–41] This difference may be related to different tail states, crystallinity and other factors.

Figure 2(a) shows the *I*–*V* curve of the interdigitated Au/Ga_2O_3/Au device in the dark and under 254 nm illumination, in which the rectification characteristic indicates a typical Schottky contact between Au and Ga_2O_3. Figure 2(b) shows the responsivity and gain spectral of the device at 20 V bias. Responsivity (R_λ) and gain (G_λ) could be calculated by[21,42]

$$R_\lambda = \frac{I_\lambda - I_d}{P_\lambda S}, \tag{1}$$

$$G_\lambda = \frac{R_\lambda hc}{\eta q \lambda}, \tag{2}$$

where I_λ is the light current, I_d is the dark current, P_λ is the intensity of the illumination, S is the effective area, h is the Planck's constant, c is the speed of light, η is the quantum efficiency (assuming the quantum efficiency is 100%), q is the elementary charge, and λ is the wavelength of illumination. The responsivity spectrum shows predominant peak (> 2.5 A/W) at 230–250 nm, and the corresponding gain is > 13. The UV-to-visible rejection ratio that is defined as the responsivity ratio at 240 nm and that at 400 nm of around 114 is achieved in the photodetector.

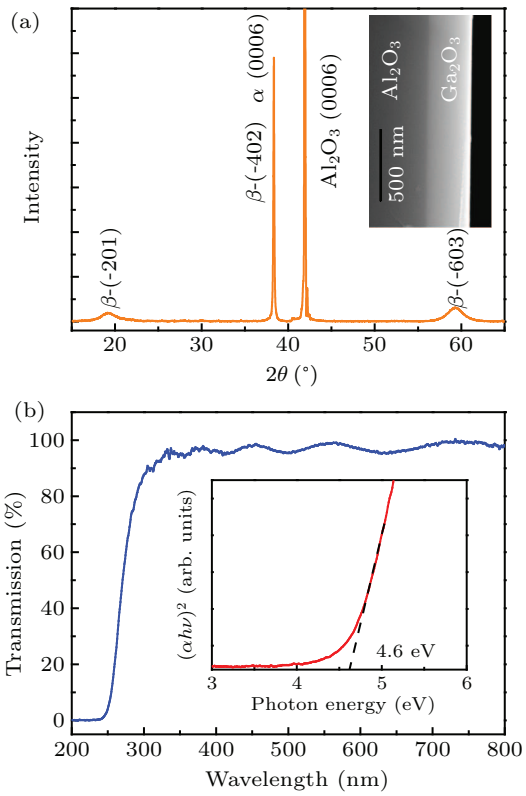


Fig. 1. (a) XRD pattern of the Ga_2O_3 film, the typical cross-sectional SEM image of the film (inset). (b) Optical transmittance spectra of the Ga_2O_3 film. The inset shows the band-gap fit.

Figure 2(c) shows the time-dependent photoresponse of the Au/Ga_2O_3/Au device to 254 nm illumination at −20 V bias. The dark current is about 1 nA and the current increases rapidly to about 4 μA once the light illuminates on the device. After removing the light, it takes more than 5 hours for the PPC current to return to the initial dark current (black line) due to the PPC effect. In order to restrain the PPC, −15 V, +10 V, +15 V, +20 V, +25 V, and +30 V pulses with duration of 500 ms were applied to the Au/Ga_2O_3/Au device. As shown in Fig. 2(c), the −15 V pulse has almost no effect on the PPC current attenuation,

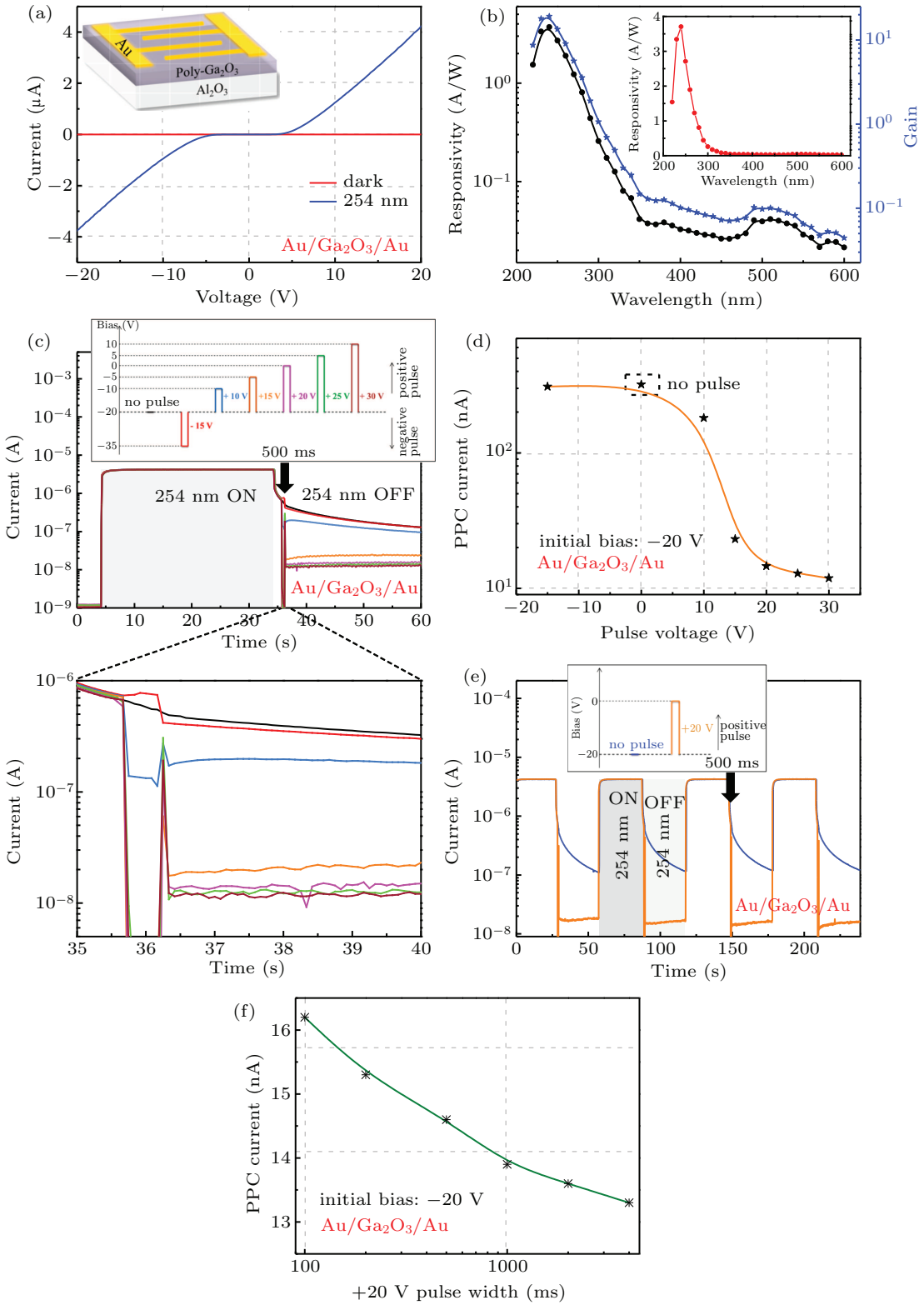


Fig. 2. (a) The *I*–*V* characteristics of the Au/Ga_2O_3/Au device in dark and under 254 nm illumination (446 μW/cm^2). The inset shows the device structure. (b) Responsivity and gain spectrum at 20 V bias in semilog scale. The inset shows the linear responsivity spectrum. (c) Time-dependent photoresponses of the device to 254 nm illumination. This includes the effect of different voltage pulses on PPC. (d) PPC current vs. the pulse voltage. (e) The time-dependent cyclic photoresponse of the device. (f) PPC current vs. the pulse width. The PPC current was measured 4 s later than the pulse voltage.

and when +10 V, +15 V, +20 V, +25 V, and +30 V pulses are applied, the PPC current drops significantly. For comparison purpose, the PPC currents measured 4 s after the end of the pulse were used to evaluate the effect of the pulse voltage on PPC suppression. Figure 2(d) shows the variation of the PPC current with the pulse voltage. The greater the applied positive pulse voltage, the more the PPC current drops. The PPC current corresponding to pulse voltages of +20 V, +25 V and +30 V drops sharply from 320 nA without pulse voltage to 14–11 nA. Taken the +20 V pulse as an example, time-

dependent photoresponse cycling showed that the pulse voltage not only suppressed PPC, but also was harmless to the stability and repeatability of photoresponse (Fig. 2(e)). When the +20 V pulse duration increases from 100 ms to 4000 ms, the corresponding PPC current decreases from 16.2 nA to 13.3 nA (Fig. 2(f)). Obviously, applying a pulse voltage can make the response recovery time of the device reach 100 ms. Note that, as shown in Fig. 2(c), after the pulse voltage is removed, the current has a short process of rapid rise. This may be related to the rapid extraction/injection process of electrons in the Schottky junction region when the bias at both ends of the Schottky junction changes instantaneously.

Figure 3(a) shows the *I*–*V* characteristics of the interdigitated Al/Ga_2O_3/Al device in the dark and under 254 nm illumination, in which a linear *I*–*V* curve indicated that Al and Ga_2O_3 film formed a typical Ohmic contact. The responsivity is 7.9 A/W at 254 nm, and the corresponding gain is 41. Figure 3(b) shows the time-dependent photoresponses of the Al/Ga_2O_3/Al device to 254 nm illumination at −20 V bias, in which one can also see an obvious PPC effect. But unlike the Au/Ga_2O_3/Au device, the pulse voltages of −15 V, +20 V and +30 V (pulse duration was also 500 ms) have almost no contribution to PPC current attenuation (Fig. 3(b)).

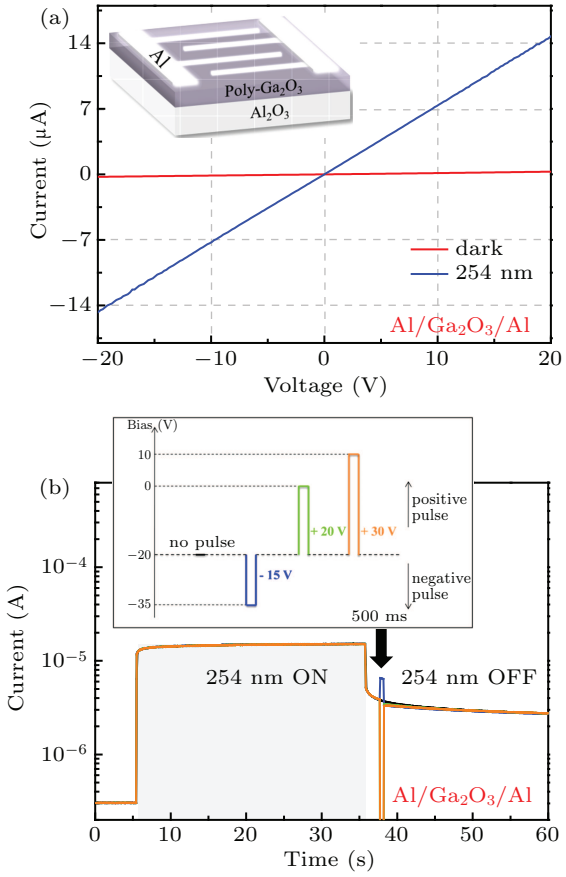


Fig. 3. (a) The *I*–*V* characteristics of the Al/Ga_2O_3/Al device in dark and under 254 nm illumination (44 6 μW/cm^2). The inset shows the device structure. (b) Time-dependent photoresponses of the device to 254 nm illumination.

In our previous report, the gain and PPC in the Ga_2O_3 photoconductor were related to the ionized oxygen vacancies (V_o^{2+}).[21] When the electron on neutral deep level V_o is excited by light ($V_o \rightarrow V_o^{2+} + 2e$) there will be an energy barrier generated between the shallow level V_o^{2+} and the electrons in the conduction band because the surrounding bonds near V_o are released outward, which prevent V_o^{2+} and electrons from quick neutralization.[22,24,26,43,44] Therefore, after the conduction band electrons paired with the long-lived V_o^{2+} are collected by the external circuit, the external circuit will continue to replenish electrons to maintain the electrical neutrality of the system until the positively charged V_o^{2+} are neutralized with the electrons. Therefore, multiple carriers are collected by absorbing one photon, and a high photocurrent (gain) is achieved. As a result, Ga_2O_3 photoconductor will remain conductive even the illumination is removed (PPC) due to the high electron density in the conduction band. In addition, according to the theories of Deak *et al.*[10] and Ryu *et al.*,[45] V_o have a trap trapping effect on valence band holes ($V_o + 2h^+ \rightarrow V_o^{2+}$) generated by light excitation. This is similar to the effect of the aforementioned photoionized oxygen vacancy ($V_o \rightarrow V_o^{2+} + 2e$) on the gain and PPC of the Ga_2O_3 photoconductor.

It is known that Au/Ga_2O_3/Au device is composed of two Schottky junctions, in which one Schottky junction is always reverse-biased and the other is forward-biased. In order to verify whether the forward-biased Schottky junction or the reverse-biased Schottky junction made more contribution to PPC suppression, we fabricated an Al/Ga_2O_3/Au device with Al and Au square electrodes. Because the Schottky contact is at the Au electrode and the Ohmic contact is at the Al electrode, the *I*–*V* curve of the Al/Ga_2O_3/Au device in dark shows significant rectification characteristics (Fig. 4(a)). As shown in Fig. 4(b), when the Ga_2O_3/Au Schottky junction is forward-biased with a bias of +20 V, a −20 V pulse with duration of 500 ms is applied to the device, and the PPC current is almost unaffected. On the contrast, when the Ga_2O_3/Au Schottky junction is reverse-biased with the bias of −20 V, the PPC current is reduced dramatically once a +20 V pulse with 500 ms duration is applied to the device, as shown in Fig. 4(c). Therefore, the pulse voltage will take effect upon suppressing PPC only in reverse biased Ga_2O_3/Au Schottky junction.

As we all know, the characteristics of Schottky photodetector are mainly related to the Schottky barrier, especially when the junction is under a reverse bias. In the metal/Ga_2O_3 Schottky junction, the metal/Ga_2O_3 interface trap and the hole self-trapped trap near the Schottky junction can trapping photo-generated holes, which are considered to be two main mechanisms that may reduce the height of the Schottky barrier.[46–48] If the interface trap state trapping holes is the main mechanism of PPC in our Schottky device. Then, only under the forward bias, it is almost possible to make the electrons tend to the interface to recombine the trapped holes

and achieve the effect of suppressing PPC. However, our experiments show that applying +10 V and +15 V pulses can suppress PPC, and the bias on the Schottky junction at this time is −10 V and −5 V under reverse bias (Fig. 2(c)). The self-trapped hole model near the Schottky junction believes that the electron–phonon coupling of the lattice is so strong that the holes in the valence band induce local distortion of the ion positions in the lattice, thereby generating an electrostatic potential that locates the holes.[48] Since the self-trapping of holes is an inherent material property, this model will produce gains in any combination of Schottky metal and Ga_2O_3 surface orientations.[48] However, in our previous work, as the annealing temperature of the Ga_2O_3 film increased to 800 °C, the corresponding MSM Schottky device's responsivity (gain) at 254 nm decreased from 136 A/W (706) to 3×10^{-4} A/W (0.0016).[23] Obviously, these devices do not all show significant gains, that is, the gains are not all greater than 1.

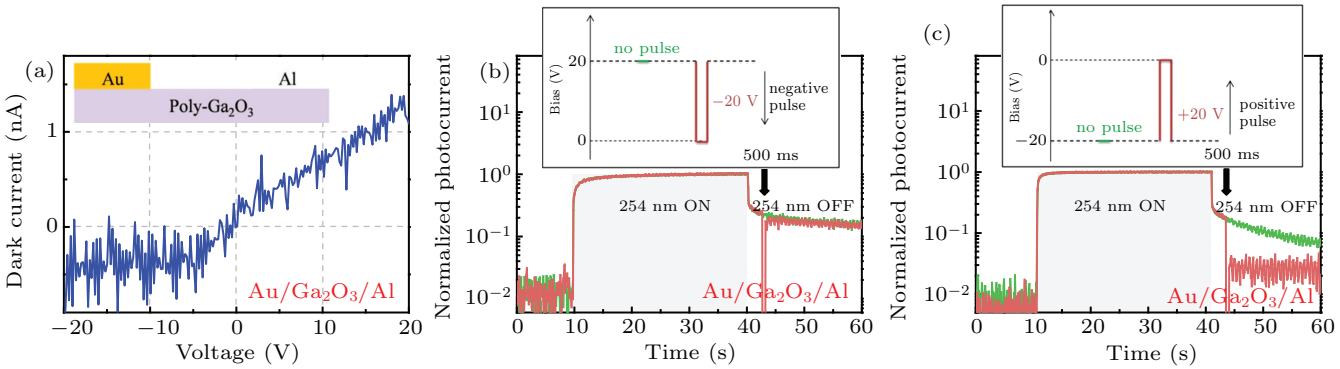


Fig. 4. (a) The *I*–*V* characteristics of Au/Ga_2O_3/Al device with square electrodes in dark. The inset shows the device structure. Panels (b) and (c) show the time-dependent photoresponses of the device to 254 nm illumination under forward bias and reverse bias, respectively. The −20 V and +20 V pulses were selected for demonstration, respectively.

In fact, our previous work and literature results show that as the oxygen vacancy concentration in Ga_2O_3 decreases, the responsivity (gain) and PPC of the Schottky device decrease and weaken, respectively.[4,23,25,49] Therefore, the gain and PPC of our Ga_2O_3 Schottky photodetectors are more likely to be related to the oxygen vacancy in Ga_2O_3.

Generally, the effective Schottky barrier height is used to measure the ability of the Schottky barrier to block carriers. If the effective Schottky barrier height is higher, it means that it is more difficult for carriers to cross the barrier, and vice versa, it is easier to cross the barrier. The effective Schottky barrier height is affected by the mirror force and the tunneling effect. As we all know, the donor concentration (for n-type semiconductors) affects the strength of the image force and tunneling effect. If the donor concentration is higher, the image force and tunneling effect are stronger. In our experiment, due to the large resistance of the Ga_2O_3 film, it is difficult to obtain the carrier concentration in the sample by Hall. According to literature reports, the carrier concentration of undoped Ga_2O_3 samples in the dark is much lower than 10^{16} cm^{-3}.[25,31] Therefore, the donor concentration of the undoped Ga_2O_3 sample in the dark is much lower than 10^{16} cm^{-3}. However, the ultraviolet light excites the electrons in the valence band and the original neutral V_o to the conduction band, leaving valence band holes and shallow donor V_o^{2+}.[21–26] At the same time, the original neutral V_o traps the valence band holes generated by the light excitation and transforms into V_o^{2+}.[10,45] Therefore, under ultraviolet light, the donor concentration in the Ga_2O_3 sample increases. According to literature reports, the concentration of oxygen vacancies in Ga_2O_3 is generally 10^{16}–10^{18} cm^{-3}.[12–15] If we assume that the concentration of oxygen vacancies in our Ga_2O_3 film is about 10^{17} cm^{-3}, the donor concentration in Ga_2O_3 is about 10^{17} cm^{-3} under ultraviolet light. Therefore, it can be understood that the donor concentration increases under light, which will cause the image force and tunneling effect to become stronger, so the effective Schottky barrier height is reduced more, and the carriers are more likely to pass through the Schottky junction.

Based on the above considerations, combined with the energy band diagram of the reverse-biased Schottky junction (Fig. 5), the gain and PPC in the reverse-biased Schottky device can be understood as follows. In the initial dark (Fig. 5(a)), the neutral V_o in Ga_2O_3 is at a deep level. Under ultraviolet light illumination (Fig. 5(b)), electrons in both the valence band and V_o are excited to the conduction band, leaving valence band holes and shallow donor V_o^{2+}.[21–26] Meanwhile, the V_o have a trap trapping effect on the valence band holes generated by light excitation.[5,45] Neutral V_o is converted to positively charged V_o^{2+}, so the donor concentration increases, the image force and tunneling effect become stronger, resulting in a greater reduction in the effective Schottky barrier height, and electrons are more easily transported from the metal to Ga_2O_3. As the effective Schottky barrier height is reduced, the positively charged V_o^{2+} in Ga_2O_3 can more easily induce the continuous injection of electrons from the contacts to maintain electrical neutrality in the quasi-neutral region, and ultimately generate high

photocurrent (gain). Once the illumination ends (Fig. 5(c)), the conduction band electrons and valence band holes in the Schottky junction will quickly recombine or be swiped away. However, due to the depletion of electrons in the Schottky junction, the shallow donor V_o^{2+} cannot be quickly neutralized, and a high donor concentration is still maintained in the Schottky junction. Therefore, the effective Schottky barrier height is still low, resulting in an obvious PPC.

Based on the above experimental results and our model, the suppression effect of the pulse voltage on the PPC in the reverse-biased Schottky device can be understood as follows. Take the application of +20 V pulse as an example (Fig. 5(d)). Due to the pulse voltage, the bias across the Schottky junction changes from −20 V to 0 V. According to formula (3), using the above estimated donor concentration in Ga_2O_3 of 10^{17} cm^{-3} under illumination, the change in Schottky barrier width x_d before and after the bias can be calculated by[50]

$$x_d = \left\{ \frac{2\varepsilon_r \varepsilon_0 (V_D - V)}{qN_D} \right\}^{1/2}, \tag{3}$$

where q is the unit electronic charge, N_D is the donor concentration, ε_r is the relative permittivity of Ga_2O_3, ε_0 is the vacuum permittivity, V_D is the built-in potential difference (about 1 V) under 0 V bias, and V is the applied bias. Calculations show that the width of the depletion region is 48 nm and 11 nm before and when the pulse is applied. Therefore, when a pulse is applied, the part V_o^{2+} that was previously in the depletion region will be located outside the depletion region. The high electron concentration outside the depletion region is easier to neutralize these V_o^{2+}. After the pulse is removed (Fig. 5(e)), the bias is restored to −20 V, but the V_o^{2+} concentration in the depletion region is significantly lower than that before the pulse is applied. Therefore, the height of the effective Schottky barrier is remarkably restored, and the Ga_2O_3/Au Schottky junction has a stronger blocking effect on electrons. Therefore, the PPC in the Ga_2O_3/Au photodetector is suppressed. Larger the positive voltage pulse or longer the pulse duration, more V_o^{2+} in the previous depletion region can be neutralized with electrons and more effective the attenuation of PPC will be (Figs. 2(c), 2(d), and 2(f)).

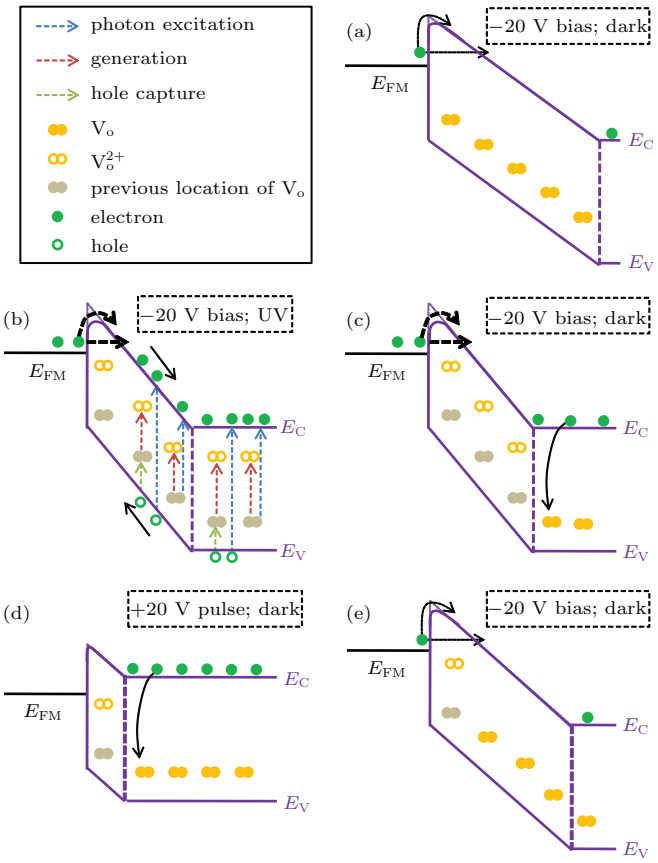


Fig. 5. Schematic diagram of the energy band at Au/Ga_2O_3 Schottky junction: (a) initial in dark; (b) under illumination; (c) after illumination has removed; (d) applying a +20 V pulse voltage; (e) after the pulse voltage ends.

Table 1 shows some important parameters of Ga_2O_3 photodetectors that have been reported. With the responsivity provided in the literature, the gain can be calculated. Our MSM devices have high responsivity and gain. More importantly, the pulse voltage suppression PPC makes the response recovery time of the device 0.1 s, so it achieves a fast response recovery speed while maintaining high responsivity (gain).

Table 1. Comparison of the photoresponse parameters between the Ga_2O_3 based photodetectors.

Ga_2O_3	Structure of device	Recovery time (s)	Responsivity (A/W)	Gain	Ref.
Single crystal	heterojunction	219.19	39.3	204.36	[20]
Single crystal	MSM	∼ 15	29.8	154.96	[51]
Single crystal	MSM	0.41/12.23	8.41	43.7	[52]
Substrate	Schottky	2.4×10^{-2}	1.48×10^{-2}	–	[6]
Nanostructure film	Schottky	6×10^{-5}	2.9×10^{-3}	0.015	[33]
Nanostructure film	MSM	∼ 100	–	–	[53]
Film	MSM	1.2/32.68	1.45	7.54	[58]
Film	MSM	0.1	1.13×10^{-3}	0.006	[54]
Film	MSM	1.02/16.61	–	–	[55]
Film	MSM	0.022	8×10^{-2}	0.42	[57]
Film	MSM	> 10	5	26	[56]
Film	MSM	2.0	9.63	–	[9]
Film	MSM	0.1	> 2.5 A/W	> 13	this work

4. Conclusions

In summary, Ga_2O_3/Au Schottky photodetectors suffer from severe PPC effects. However, when the Schottky junction is in reverse bias, the PPC can be suppressed by applying a positive pulse voltage. As a result, a Ga_2O_3 photodetector with high gain (> 13) and fast response recovery speed (0.1 s) is obtained. The physical mechanism of gain and PPC is attributed to the decrease of the effective Schottky barrier height due to the strong mirror force and tunneling effect caused by the long lifetime V_o^{2+} in the Schottky junction. The positive pulse voltage will temporarily reduce the width of the depletion region, so that the V_o^{2+} in the previous depletion region is neutralized by the high concentration of electrons, thus suppressing PPC. Our research proposes a feasible solution to suppress PPC in Ga_2O_3 Schottky photodetectors while maintaining high gain, and can deepen the understanding of the mechanism of gain and PPC in similar devices.

References

[1] Pearton S J, Yang J, Cary IV P H, Ren F, Kim J, Tadjer M J and Mastro M A 2018 *Appl. Phys. Rev.* **5** 011301
[2] Chen M, Zhang Z, Zhan R, She J, Deng S, Xu N and Chen J 2021 *Applied Surface Science* **554** 149619
[3] Fan M, Cao L, Xu K and Li X 2021 *J. Alloys Compd.* **853** 157080
[4] Xu J, Zheng W and Huang F 2019 *J. Mater. Chem. C* **7** 8753
[5] Hou X, Zou Y, Ding M, Qin Y, Zhang Z, Ma X, Tan P, Yu S, Zhou X, Zhao X, Xu G, Sun H and Long S 2021 *J. Phys. D: Appl. Phys.* **54** 043001
[6] Tan P, Zhao X, Hou X, Yu Y, Yu S, Ma X, Zhang Z, Ding M, Xu G, Hu Q, Gao N, Sun H, Mu W, Jia Z, Tao X and Long S 2021 *Adv. Opt. Mater.* **9** 2100173
[7] Yadav M K, Mondal A, Shringi S, Sharma S K and Bag A 2020 *Semicond. Sci. Technol.* **35** 085009
[8] Yu Y T, Xiang X Q, Zhou X Z, Zhou K, Xu G W, Zhao X L and Long S B 2021 *Chin. Phys. B* **30** 067302
[9] Zhao Y, Zang J H, Yang X, Chen X X, Chen Y C, Li K Y, Dong L and Shan C X 2021 *Chin. Phys. B* **30** 078504
[10] Deak P, Ho Q D, Seemann F, Aradi B, Lorke M and Frauenheim T 2017 *Phys. Rev. B* **95** 075208
[11] Kyrtsos A, Matsubara M and Bellotti E 2017 *Phys. Rev. B* **95** 245202
[12] Zhang Z, Farzana E, Arehart A R and Ringel S A 2016 *Appl. Phys. Lett.* **108** 052105
[13] Hajnal Z, Miro J, Kiss G, Reti F, Deak P, Herndon R C and Kuperberg J M 1999 *J. Appl. Phys.* **86** 3792
[14] Zacherle T, Schmidt P C and Martin M 2013 *Phys. Rev. B* **87** 235206
[15] Huang S S, Lopez R, Paul S, Neal A T, Mou S, Houng M P and Li J V 2018 *Jpn. J. Appl. Phys.* **57** 091101
[16] Aller H T, Yu X, Wise A, Howell R S, Gellman A J, McGaughey A J H and Malen J A 2019 *Nano Lett.* **19** 8533
[17] Zhang D, Zheng W, Lin R, Li Y and Huang F 2019 *Adv. Funct. Mater.* **29** 1900935
[18] Harada T, Ito S and Tsukazaki A 2019 *Sci. Adv.* **5** eaax5733
[19] Hao S J, Hetzl M, Schuster F, Danielewicz K, Bergmaier A, Dollinger G, Sai Q L, Xia C T, Hoffmann T, Wiesinger M, Matich S, Aigner W and Stutzmann M 2019 *J. Appl. Phys.* **125** 105701
[20] Kong W Y, Wu G A, Wang K Y, Zhang T F, Zou Y F, Wang D D and Luo L B 2016 *Adv. Mater.* **28** 10725
[21] Zhou H, Cong L, Ma J, Li B, Chen M, Xu H and Liu Y 2019 *J. Mater. Chem. C* **7** 13149)
[22] Han Z, Liang H, Huo W, Zhu X, Du X and Mei Z 2020 *Adv. Opt. Mater.* **8** 1901833
[23] Zhou H, Cong L, Ma J, Chen M, Song D, Wang H, Li P, Li B, Xu H and Liu Y 2020 *J. Alloys Compd.* **847** 156536
[24] Ahn J, Ma J, Lee D, Lin Q, Park Y, Lee O, Sim S, Lee K, Yoo G and Heo J 2021 *ACS Photonics* **8** 557
[25] Cui S, Mei Z, Zhang Y, Liang H and Du X 2017 *Adv. Opt. Mater.* **5** 1700454
[26] Jeon S, Ahn S E, Song I, Kim C J, Chung U I, Lee E, Yoo I, Nathan A, Lee S, Robertson J and Kim K 2012 *Nat. Mater.* **11** 301
[27] Hou Q, Wang X, Xiao H, Wang C, Yang C, Yin H, Deng Q, Li J, Wang Z and Hou X 2011 *Appl. Phys. Lett.* **98** 102104
[28] Wang Y, Liao Z, She G, Mu L, Chen D and Shi W 2011 *Appl. Phys. Lett.* **98** 203108
[29] Liu K, Sakurai M, Aono M and Shen D 2015 *Adv. Funct. Mater.* **25** 3157
[30] Hou M, So H, Suria A J, Yalamarthy A S and Senesky D G 2017 *IEEE Electron Device Lett.* **38** 56
[31] Qiao B, Zhang Z, Xie X, Li B, Chen X, Zhao H, Liu K, Liu L and Shen D 2021 *J. Mater. Chem. C* **9** 4039
[32] Pratiyush A S, Krishnamoorthy S, Solanke S V, Xia Z, Muralidharan R, Rajan S and Nath D N 2017 *Appl. Phys. Lett.* **110** 221107
[33] Chen X, Liu K, Zhang Z, Wang C, Li B, Zhao H, Zhao D and Shen D 2016 *ACS Appl. Mater. Interfaces* **8** 4185
[34] Oshima T, Okuno T and Fujita S 2007 *Jpn. J. Appl. Phys.* **46** 7217
[35] Ghose S, Rahman S, Hong L, Rojas-Ramirez J S, Jin H, Park K, Klie R and Droopad R 2017 *J. Appl. Phys.* **122** 095302
[36] Chen Y C, Lu Y J, Liu Q, Lin C N, Guo J, Zang J H, Tian Y Z and Shan C X 2019 *J. Mater. Chem. C* **7** 2557
[37] Heinemann M D, Berry J, Teeter G, Unold T and Ginley D 2016 *Appl. Phys. Lett.* **108** 022107
[38] Kim J, Sekiya T, Miyokawa N, Watanabe N, Kimoto K, Ide K, Toda Y, Ueda S, Ohashi N, Hiramatsu H, Hosono H and Kamiya T 2017 *NPG Asia Mater.* **9** e359
[39] Chen Y, Lu Y, Liao M, Tian Y, Liu Q, Gao C, Yang X and Shan C 2019 *Adv. Funct. Mater.* **29** 1906040
[40] Li K H, Kang C H, Min J H, Alfaraj N, Liang J W, Braic L, Guo Z, Hedhili M N, Ng T K and Ooi B S 2020 *ACS Appl. Mater. Interfaces* **12** 53932
[41] Wang Y, Yang Z, Li H, Li S, Zhi Y, Yan Z, Huang X, Wei X, Tang W and Wu Z 2020 *ACS Appl. Mater. Interfaces* **12** 47714
[42] Li L, Chen H, Fang Z, Meng X, Zuo C, Lv M, Tian Y, Fang Y, Xiao Z, Shan C, Xiao Z, Jin Z, Shen G, Shen L and Ding L 2020 *Adv. Mater.* **32** 1907257
[43] Lany S and Zunger A 2005 *Phys. Rev. B* **72** 035215
[44] Janotti A and Van de Walle C G 2005 *Appl. Phys. Lett.* **87** 122102
[45] Ryu B, Noh H K, Choi E A and Chang K J 2010 *Appl. Phys. Lett.* **97** 022108
[46] Xu Y, Chen X, Zhou D, Ren F, Zhou J, Bai S, Lu H, Gu S, Zhang R, Zheng Y and Ye J 2019 *IEEE Trans. Electron. Dev.* **66** 2276
[47] Qin Y, Li L, Zhao X, Tompa G S, Dong H, Jian G, He Q, Tan P, Hou X, Zhang Z, Yu S, Sun H, Xu G, Miao X, Xue K, Long S and Liu M 2020 *ACS Photonics* **7** 812
[48] Armstrong A M, Crawford M H, Jayawardena A, Ahyi A and Dhar S 2016 *J. Appl. Phys.* **119** 103102
[49] Guo D Y, Wu Z P, An Y H, Guo X C, Chu X L, Sun C L, Li L H, Li P G and Tang W H 2014 *Appl. Phys. Lett.* **105** 023507
[50] Sze S M and Ng K K 2007 *Physics of Semiconductor Devices*, 3rd ed. (Hoboken: Wiley)
[51] Oh S, Kim C and Kim J 2018 *ACS Photonics* **5** 1123
[52] Qian L X, Liu H Y, Zhang H F, Wu Z H and Zhang W L 2019 *Appl. Phys. Lett.* **114** 113506
[53] Guo D, Wu Z, Li P, Wang Q, Lei M, Li L and Tang W 2015 *RSC Adv.* **5** 12894
[54] Shen H, Yin Y, Tian K, Baskaran K, Duan L, Zhao X and Tiwari A 2018 *J. Alloys Compd.* **766** 601
[55] Guo D, Wu Z, Li P, An Y, Liu H, Guo X, Yan H, Wang G, Sun C, Li L and Tang W 2014 *Opt. Mater. Express* **4** 1067
[56] Ahn S, Ren F, Oh S, Jung Y, Kim J, Mastro M A, Hite J K, Eddy C R and Pearton S J 2016 *J. Vac. Sci. Technol. B* **34** 041207
[57] Fan M, Lu Y, Xu K, Cui Y, Cao L and Li X 2020 *Applied Surface Science* **509** 144867
[58] Oh S, Jung Y, Mastro M A, Hite J K, Eddy Jr C R and Kim J 2015 *Opt. Express* **23** 28300